Published online August 1, 2007

Vadose Zone Journal ORIGINAL RESEARCH

Nitrous Oxide Fluxes from Cultivated Areas and Rangeland: U.S. High Plains

Edwin P. Weeks* and Peter B. McMahon

Concentration profiles of N_2O, a greenhouse gas, and the conservative trace gases SF_6 and the chlorofluorocarbons CFC-11, CFC-12, CFC-113, and were measured periodically through thick vadose zones at nine sites in the U.S. High Plains. The CFC and SF_6 measurements were used to calibrate a one-dimensional gas diffusion model, using the parameter identification program UCODE. The calibrated model was used with N_2O measurements to estimate average annual N_2O flux from both the root zone and the deep vadose zone to the atmosphere. Estimates of root-zone N_2O fluxes from three rangeland sites ranged from near 0 to about 0.2 kg N_2O-N ha^{-1} yr^{-1}, values near the low end of the ranges determined for native grass from other studies. Estimates of root-zone N_2O fluxes from two fields planted to corn (*Zea mays* L.) of about 2 to 6 kg N_2O-N ha^{-1} yr^{-1} are similar to those determined for corn in other studies. Estimates of N_2O flux from Conservation Reserve grassland converted from irrigated corn indicate that production of N_2O is substantially reduced following conversion from cropland. Small N_2O fluxes from the water table or from deep in the vadose zone occurred at three sites, ranging from 0.004 to 0.02 kg N_2O-N ha^{-1} yr^{-1}. Our estimates of N_2O flux represent space- and time-averaged values that should be useful to more fully evaluate the significance of instantaneous point flux measurements.

ABBREVIATIONS: CAL, Central High Plains Conservation Reserve Program site; CFC, chlorofluorocarbon; CHP, Central High Plains; CNG, Central High Plains rangeland site; EEC, equivalent equilibrium concentration in water-vapor-saturated air; GNT, Northern High Plains irrigated corn site at Grant, NB; IMP, Northern High Plains rangeland site; JRW, Southern High Plains irrigated cotton site in Cochran County, TX; MPL, Southern High Plains irrigated cotton site at Maple, TX; MWR, Southern High Plains rangeland site; NHP, Northern High Plains; SHP, Southern High Plains; UMA, Northern High Plains irrigated corn site at Yuma, CO.

The USGS has collected data on trace gas concentrations, including the chlorofluorocarbons CFC-12, CFC-11, CFC-113, SF_6, and N_2O at several depths in the deep vadose zone at each of nine sites underlain by the High Plains Aquifer. The CFC and SF_6 data provide an opportunity to further evaluate the field technique of Weeks et al. (1982) for identifying the gas-diffusion transport properties of thick sequences of unsaturated materials, using a larger range of atmospheric tracers than were available at the time of that study. Identification of diffusive transport properties of vadose zone materials is of importance to a broad range of environmental studies, including most notably those involving the soil–atmosphere exchange of greenhouse gases and those involved in risk assessment of and bioremediation potential for sites contaminated by volatile organic compounds. Of a variety of field techniques available for the determination of these transport properties, as reviewed by Werner et al. (2004), the method described here is most suitable for evaluations of large volumes of material.

U.S. Geological Survey, Box 25046, MS 413, Lakewood, CO 80225.
Received 8 Nov. 2006. *Corresponding author (epweeks@usgs.gov).

Vadose Zone J. 6:496–510
doi:10.2136/vzj2006.0164

Availability of the N_2O data, coupled with the identified diffusive transport properties based on analysis of the CFC data, provides a means of estimating long-term average production rates for the gas, both in the active root zone and from depth in the vadose zone. Nitrous oxide is of environmental concern because it acts both as a greenhouse gas and as an agent in the destruction of stratospheric ozone (Cicerone, 1987). Its concentration has been increasing in the atmosphere by about 0.24% yr^{-1} for the last 25 yr or so. Nitrification and denitrification of N-based fertilizers within the soil zone are considered to be a major source of this increase (Kroeze et al., 1999, p. 6). In addition, Ronen et al. (1988) indicated that N_2O may be produced by denitrification at the water table under heavily fertilized fields, and that this N_2O may provide a significant diffusive flux through the vadose zone to the land surface.

Estimation of root-zone N_2O flux from rangeland and irrigated crops from the 450,000-km^2 area underlain by the High Plains Aquifer should prove useful in evaluating this source of N_2O to the atmosphere. The detection of N_2O production at depth in the vadose zone or at the water table will further elucidate sources of the gas. Also, the technique may be of interest to others involved with estimation of soil–atmosphere greenhouse gas exchange in areas underlain by deep vadose zones, as the method provides estimates of seasonal or long-term spatial average production rates. These might prove particularly useful, as the main measurement techniques used for determining N_2O emissions from soils are by measurements at the land surface, either through the use of chambers (Eichner, 1990), or, occasionally, by micrometeorological methods (Phillips et al., 2007; Smith et al.,

1994). These measurements indicate that soil fluxes of N_2O are extremely variable in both time and space, making their integration into long-term areal averages difficult.

Materials and Methods

The nine sites used for this study include three each in the Southern (SHP), Central (CHP), and Northern High Plains (NHP), as shown in Fig. 1 (northernmost 43.67, southernmost 31.80, easternmost −96.26, westernmost −105.91) . Sites in the SHP include one in rangeland, supporting native grasses and forbs, and two that have been planted to irrigated cotton (*Gossypium hirsutum* L.). Sites in the CHP include one in rangeland and two that are adjacent to land that has been planted to irrigated corn. Both irrigated sites were converted from flood to center-pivot sprinkler irrigation in 1990 (McMahon et al., 2003). The sampling well installations are in corners of the field that are no longer irrigated, and have been planted to grass as part of the USDA Conservation Reserve Program. Sites in the NHP include one in rangeland and two planted to irrigated corn, with sampling instrumentation installed immediately adjacent to the corn fields.

The rangeland sites are all in native pasture, and support a cover of grass, forbs, and bare ground, with vegetative cover increasing from south to north. The irrigated sites were all in dryland crop production, most for many years, before irrigation. Nitrogen fertilizer applications had been minor or nonexistent before irrigation, but increased dramatically with its advent. All of the irrigated sites have experienced significant declines in water table elevation since the advent of irrigation, as listed in Table 1.

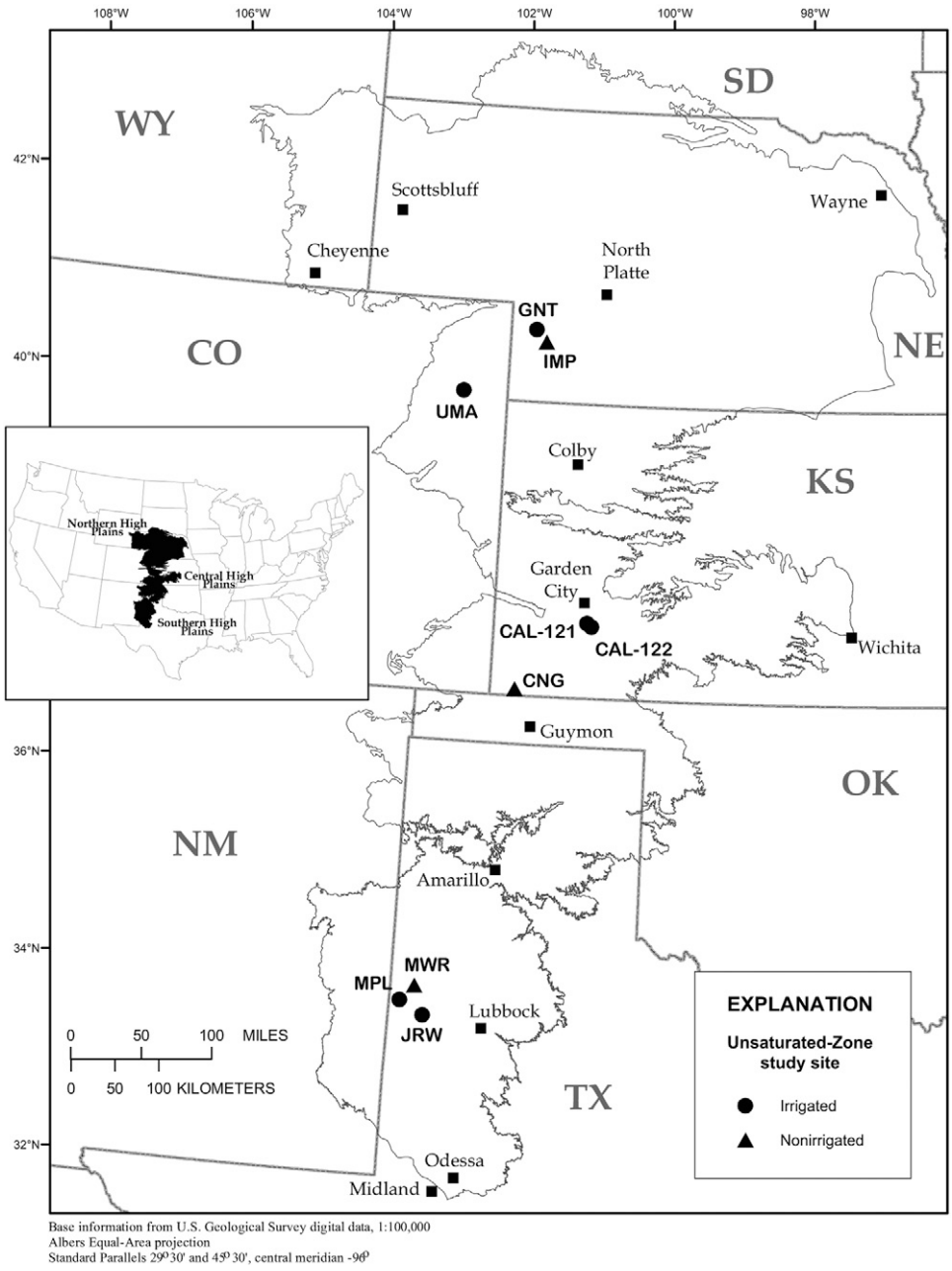

FIG. 1. Map of the High Plains Aquifer showing locations of the vadose zone study sites.

Bore holes for the installations were drilled by using a casing-advance air hammer. Drill cuttings were collected at 0.6-m intervals for particle-size analysis, and cores were collected from near land surface and at approximate 3-m intervals. Cutting samples were leached to determine NO_3 concentrations in residual pore water, in units of milligrams of N per kilogram of sediment (McMahon et al., 2006), as shown in Fig. 2. Nitrate concentrations in groundwater were also determined from water samples collected from the observation well at each site. These concentrations were converted from milligrams of N per liter of water to milligrams of N per kilogram of sediment by multiplying the concentration by 0.196 L water kg^{-1} sediment, based on a mean porosity of 0.345 and an average bulk density of 1.76 kg L^{-1}.

The bore holes were drilled to a depth of about 8 m below the water table. Site completion was accomplished by installing 3.05-m screens centered at a depth of 5 m below the water table, and backfilled with 1.7-mm sand to above the top of the screen, followed by bentonite pellets to form a seal. Four to six gas sampling ports, packed with sand, were installed at relatively uniform intervals, but adjusted on the basis of lithology at each site, and were isolated by bentonite. Observation well and gas-sampling port screen depths are shown superimposed on unsaturated-zone lithology for the nine sites in Fig. 3. Heat dissipation probes and suction lysimeters were installed at separate locations and packed with silica flour, as shown by McMahon et al. (2006). Sampling nest construction was conducted in the CHP in March to April 2000, in the SHP in May to June 2001, and in the NHP in June 2002. Four near-surface gas-sampling ports were installed

TABLE 1. Site data for the nine High Plains sites.

Site ID	Location†	Cover	Date installed	Altitude‡	MAT§	Initial water table	Final water table	Decline	Irrigation start	Center pivot	Fertilizer start
				m	°C	—— m ——		m yr^{-1}			
CNG	Kansas (CHP)	rangeland	April 2000	1035	13.2	50	50	0.0	NA¶	NA	NA
IMP	Nebraska (NHP)	rangeland	June 2002	1004	10.5	25	27.5	0.0	NA	NA	NA
MWR	Texas (SHP)	rangeland	June 2001	1166	14.2	15.5	15.5	0.0	NA	NA	NA
UMA	Colorado (NHP)	corn	June 2002	1237	10.5	33	47.5	0.32	1956	1989	1986#
GNT	Nebraska (NHP)	corn	June 2002	1034	10.5	35	45	0.34	1974	1974	1974
CAL-121	Kansas (CHP)	corn/grass	March 2000	875	11.7	27	45	0.45	1956	1990	1956
CAL-122	Kansas (CHP)	corn/grass	April 2000	875	12.4	15	45	0.90	1955	1988	1955
JRW	Texas (SHP)	cotton	June 2001	1118	14.2	33	46	0.325	1958	1991	late 1960s
MPL	Texas (SHP)	cotton	June 2001	1190	14.2	35.75	42	0.15	1958	1991	1958

† SHP, Southern High Plains; CHP, Central High Plains; NHP, Northern High Plains.
‡ Datum is NGVD29.
§ Mean annual air temperature.
¶ NA = not applicable.
# First records available, but is thought to have begun earlier.

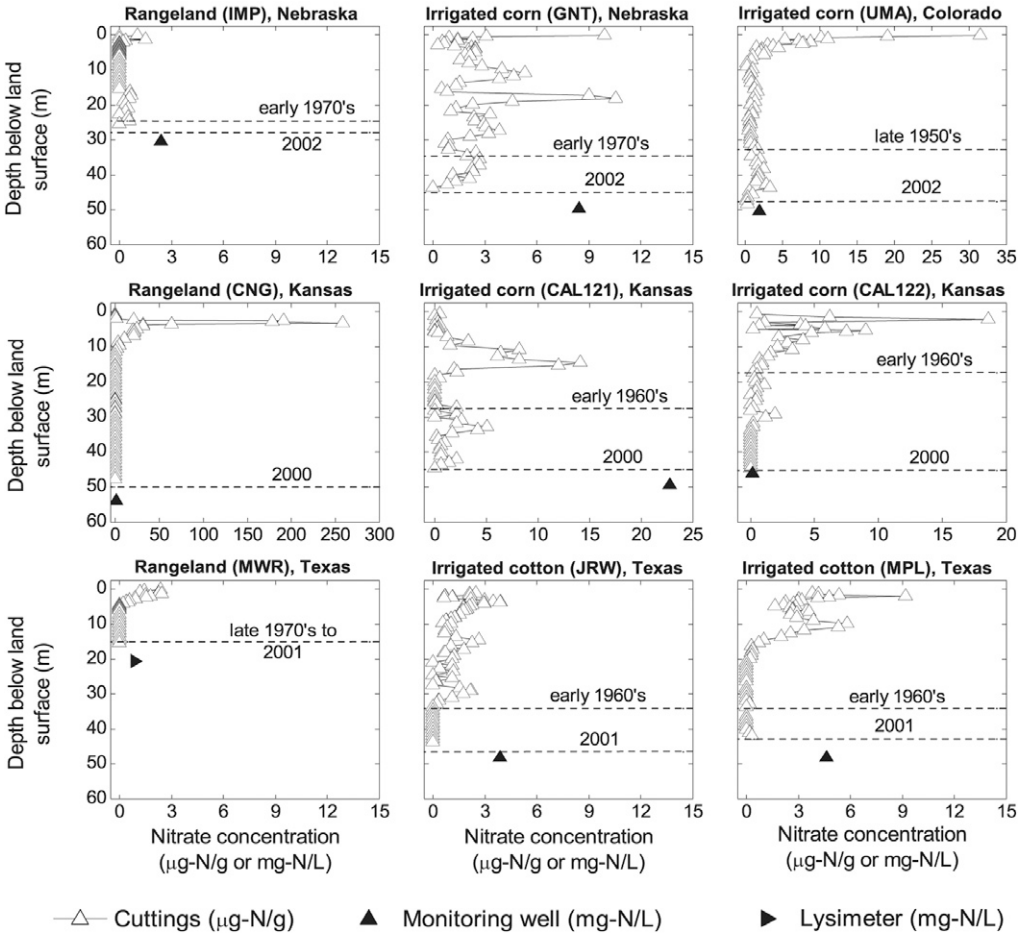

FIG. 2. Profiles of NO_3 extracted from vadose zone sediment cuttings and NO_3 concentrations in groundwater (after McMahon et al., 2006). Note the break in the *x*-axis scale at the UMA and GNT sites. Horizontal dashed lines in each plot represent water table depths at indicated times. In groundwater, concentrations plotted on a mass basis were calculated from concentrations measured on a volume basis (in parentheses) and porosity and bulk density data from McMahon et al. (2003). Zones of high NO_3 are commonly associated with indicated zones of N_2O production.

in 2003 at the three sites in the NHP at intervals of 0.3 m below the land surface to provide greater near-surface detail.

Gas samples for analysis of CFCs and SF_6 were collected from the atmosphere and each of the gas sampling ports from each site in the CHP at 2, 8, and 17 mo after nest completion. Sampling for CFCs and SF_6 occurred twice each, at 8 and 13 mo at sites in the SHP and 11 and 14 mo at sites in the NHP. These samples were collected in glass ampules by purging with ultrapure N_2, pumping several volumes of air or vadose zone gas, and then flame sealing the ampule necks, as described in detail by Busenberg and Plummer (1992, p. 2258). Samples were shipped to the USGS Chlorofluorocarbon Laboratory in Reston, VA, for analysis using an electron-capture detector equipped gas chromatograph. Analytical techniques are described in detail, both for gas samples and for water samples (described below), for CFC analysis by Busenberg and Plummer (1992) and for SF_6 analysis by Busenberg and Plummer (2000).

Samples for N_2O (and CO_2, not used in this study) were collected five times at each site in the CHP, at 2, 5, 8, 17, and 30 mo after sampling nest completion. Four sets of samples were collected, at 4, 8, 13, and 25 mo, at nests in the SHP, and six sets at nests in the NHP, starting 8 mo and ending 26 mo after completion. These samples were collected in 25-mL glass bottles by first flushing the open bottles with unsaturated-zone gas for 5 min at a flow rate of about 1 L min^{-1}, sealing them with thick butyl stoppers, and then continued flushing of the sealed bottles

through a syringe needle for an additional 3 min. Nitrous oxide concentrations were determined by gas chromatography with electron-capture detection (1.8-m Porapak Q column, carrier gas was 95:5 Ar/CH_4) at the USGS laboratory in Lakewood, CO. The precision of the N_2O analysis was ±5% based on replicate analysis of samples and standards.

Unsaturated-zone gas samples collected within 6 mo of well completion, both for CFCs and SF_6 and for N_2O, showed concentrations that were more nearly those of atmospheric air than did those of subsequent samples, indicating contamination of soil gas with drilling air. Concentrations measured in samples collected later than 6 mo after construction, however, typically did not vary systematically with sampling date, indicating that drilling effects had dissipated by that time. Consequently, only those data collected later than 6 mo after well completion were used for model calibration and N_2O production estimates.

Gas samples were collected for whole gas analysis during one or two episodes at each site using procedures similar to those for collecting N_2O samples, and were analyzed at the Lakewood laboratory by gas chromatography with thermal-conductivity detection. Results of these analyses (not shown), as well as of published results for other sites in the High Plains (e.g., Thorstenson et al., 1983), indicated that the concentrations of major gases throughout the vadose zone are essentially identical to those in the atmosphere in the High Plains, and hence are well oxygenated.

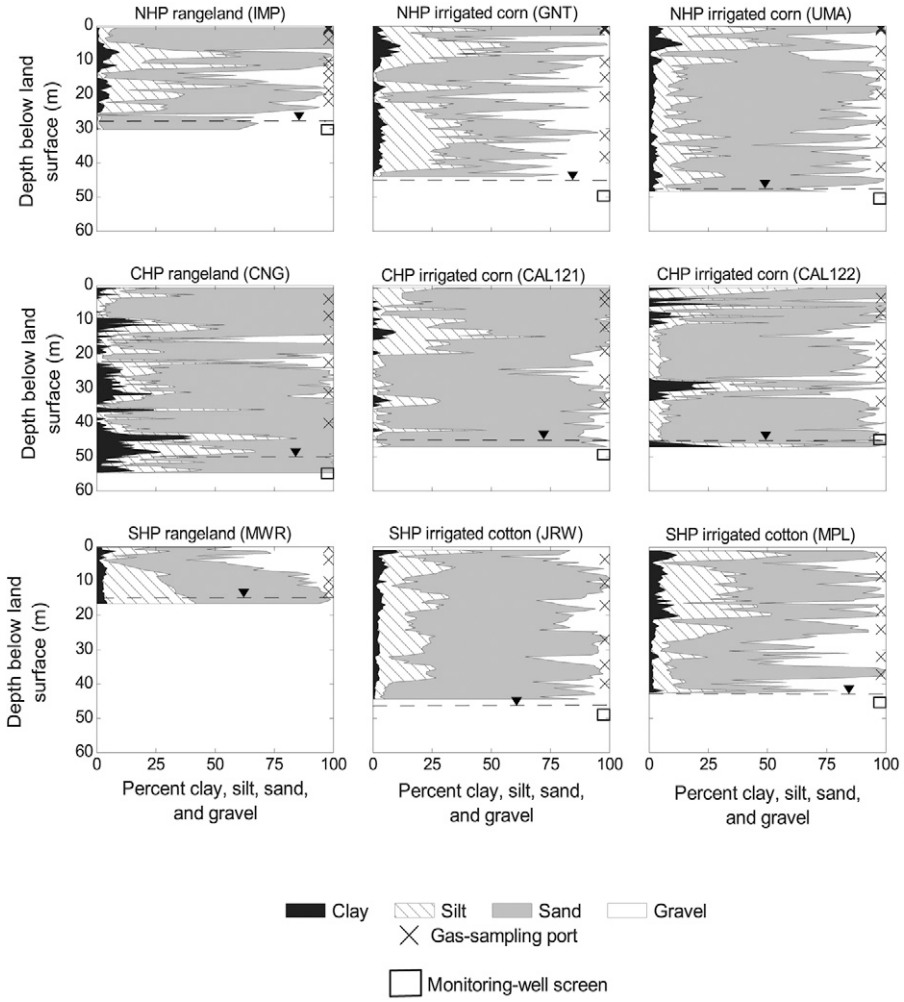

FIG. 3. Lithology and construction details for a typical High Plains vadose zone well installation; NHP = Northern High Plains; CHP = Central High Plains; SHP = Southern High Plains.

Water samples were collected at the well installations during one to four of the gas-collection episodes at each site. These samples were analyzed to determine dissolved gas concentrations of the CFCs, SF_6, N_2O, and dissolved NO_3^-. Methods of sampling and analysis for the CFCs and SF_6 are described by Busenberg and Plummer (1992, 2000), respectively, and those for dissolved N_2O and NO_3^- are described by McMahon et al. (2003). Dissolved CFC and SF_6 concentrations, converted to equivalent equilibrium concentration in water-vapor-saturated air (EEC), are substantially smaller than those measured in the deepest gas-sampling probes, as expected, and are not shown.

Gas-Phase Data Analysis

Concentration profiles for the CFCs, SF_6, and N_2O obtained for each site were processed to provide estimates of average N_2O flux for the site by application of a gas-diffusion model modified from that described in detail by Weeks et al. (1982, p. 1372–1375). Briefly, the code provides a numerical solution to the partial differential equation:

$$\tau\theta_a D_{AB}\frac{\partial C_A}{\partial z^2} = \theta'\frac{\partial C_A}{\partial t} + \alpha \qquad [1]$$

where τ is tortuosity, θ_a is drained porosity, D_{AB} is the free-air diffusion coefficient for Gas A diffusing into Gas B (air) ($L^2\ T^{-1}$), C_A is the concentration of Gas A in air ($M\ L^{-3}$), $\theta' = \theta_a + \rho_w(\theta_T - \theta_a)K_w + \rho_s(1 - \theta_T)K_wK_D$ (dimensionless), where ρ_w is the density of water ($M\ L^{-3}$), θ_T is total porosity, K_w is the gas–water partitioning coefficient ($L^3\ M^{-1}$), ρ_s is particle density ($M\ L^{-3}$), K_D is the solid–liquid distribution coefficient (dimensionless), and α is a source–sink term ($M\ L^{-3}\ T^{-1}$).

The upper boundary condition is one of specified concentration [$C_{z=0} = C(t)$], where $C(t)$ either varies as annual linear line segments (CFCs and SF_6) or is a constant (N_2O, set to 310 $nm^3\ m^{-3}$ for all simulations and analyses). Year-end concentrations of the CFCs and SF_6 in the atmosphere used for this study are those provided by the Reston Chlorofluorocarbon Laboratory (2007). Details on the syntheses of records for the various species are summarized by the International Atomic Energy Agency (2006). These concentration histories are shown in Fig. 4.

The bottom boundary (the water table) is specified as a no-flow boundary to gas diffusion. If a falling water table is specified, the bottom boundary is set to an initial water table depth. When a time step at which the decline equals one node space is reached, as computed from a uniform decline rate or read from a user-provided table, a node is added. The finite-difference grid is updated, and concentrations are advected downward through-

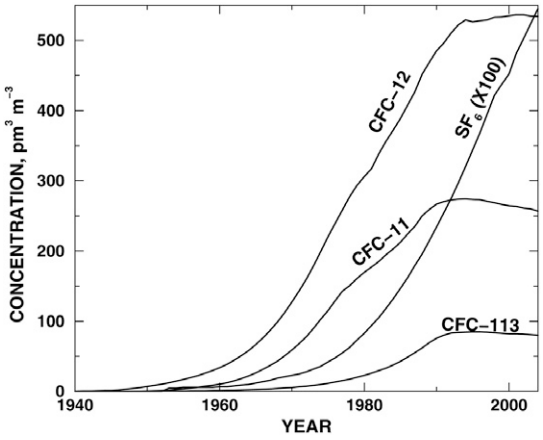

FIG. 4. Concentrations of chlorofluorocarbons CFC-11, CFC-12, CFC-113, and SF_6, in North American air as a function of time (modified from Busenberg and Plummer, 2000, Fig. 6).

out the profile by a volume equal to the air-filled pore space in one node of the layer through which the water table is declining. For simulated production at the water table, the nodes representing the production zone are moved down one node space each time a water table decline is simulated.

Initial conditions for the entire profile are set to 0 for CFCs and SF_6 by the program; for N_2O, the user provides either a constant value or a file specifying concentration for each node with depth.

The model was checked by comparison with a transport code developed by Cook and Solomon (1995). Simulations of only diffusive transport using the two codes were virtually identical. Simulations involving a falling water table were checked against those made using the transport code. For the transport code, the water table was fixed at its final depth, but a gas advection rate equal to the rate of the water table decline times the specific yield of the bottom layer was specified. Despite the different modeling approaches, the two codes provided quite similar results. In all cases, liquid-phase transport simulated using the Cook and Solomon (1995) code had only a very minor effect on the simulated profiles.

Data required to model the CFCs, SF_6, and N_2O, including their free-air diffusion and Henry's Law coefficients, are described in the Appendix. Needed site-specific data include site altitude (used to compute station pressure, m), mean annual air temperature (°C), the vadose zone thickness (m), and a discretization of the vadose zone into layers with specified depth boundaries (m). In addition, the irrigation history, the initial depth to water, and the date of first N fertilizer application are needed for the irrigated sites to establish the start of the falling water table or the start of N_2O production. Site-specific data, except those regarding layer properties, are provided in Table 1.

Materials in the vadose zone at each site are discretized into layers, based on lithology, each having uniform total porosity, water content, and drained porosity. Data used to specify layer properties and boundaries include detailed particle size analyses of cores and drill cuttings as a function of depth, and porosity and moisture content data from cores that were collected at four to eight depths at each site. The particle size data were used to divide the vadose zone into layers, and the core data to assign porosity and moisture content to each layer. Layers were selected to include either at least one set of observations or a depth interval separated from those above and below by a distinct break in slope. Thus, adjacent layers selected on the basis of geohydrology alone were often combined, based on arithmetically averaging their thickness-weighted total and air-filled porosities. For layers including one or more cores, the porosity data were applied as the average of the core values. For other layers, the porosities were assigned based on lithological similarities to those for which core data, either for that site or for other sites in the study, were available.

For all NHP sites, core data provided total and drained porosities that resulted in near-zero Millington tortuosities (defined below), that were not compatible with the CFC profile data; however, porosities and moisture characteristic curves (graphs of moisture tension vs. moisture content) had been developed from subcores of the original field cores. Heat dissipation probe data also were available from stations installed near the core depths. Indicated moisture tensions from these probes were used with the moisture-characteristic curves and the subcore porosities, which differed from those for the full cores, to estimate drained porosities that were substantially larger than those for the original cores, and these values were used for all NHP site models.

Model Calibration

Initial model calibration was achieved by trial-and-error variation of tortuosity in selected vadose zone layers to achieve an overall match to the three CFC profiles and the SF_6 profile, based on their individual free-air diffusivities and solubilities, as described in the Appendix. Calibration was initiated by assigning tortuosity as computed from the Millington (1959) equation:

$$\tau = \theta_a^{1/3}\left(\frac{\theta_a}{\theta_T}\right)^2 \qquad [2]$$

and modifying tortuosities to obtain a good visual fit. Model calibration was later redone using the parameter-identification program UCODE (Poeter and Hill, 1998). Briefly, this program uses a modified Gauss–Newton method to adjust calibration parameters, in this case layer tortuosities, to minimize the sum of squares of the (weighted) differences between measured and simulated values of specified modeled variables, in this case concentrations of the four gas species, each normalized to its interpolated concentration in the atmosphere at the time of sampling.

Model Application

The UCODE-calibrated tortuosities for the layered systems at each site were used to estimate long-term annual rates of N_2O production (the α term in Eq. [1]) since the last land use change in one or more zones by using UCODE to compute production rates that minimize the sum-of-squares difference between measured and simulated N_2O concentrations. Production zones were selected based on the shapes of the N_2O profiles.

Production at only a constant rate in the root zone will result in a constant N_2O concentration with depth below its base. Root-zone N_2O production, however, is typically seasonally episodic, resulting in concentrations below the root zone that vary seasonally about a mean value. These variations dampen with depth to achieve a constant profile that reflects the effects

of average annual root-zone production. Based on diffusion theory, the depth of complete damping is approximately reached at three times the diffusive damping depth (Campbell, 1973), determined as $\tau\theta_a D_{N_2O-Air}/\theta'$. Based on calibration results (Table 2) and N_2O diffusivity in air and solubility in water, as described in the Appendix, the damping depth for N_2O diffusion should be about 5 m, indicating that N_2O profiles should be constant with depth below a depth of about 15 m, and that the profile below that depth can be analyzed to determine an average annual production rate.

A source zone at depth providing N_2O production is indicated by a monotonic increase in concentration with depth above the source zone, and a break in slope at its location, while a relatively uniform slope through the full thickness of the vadose zone indicates production at or near the water table. Most indicated production zones correspond with zones of high NO_3 concentrations in soil water (Fig. 2), providing additional evidence for their selection.

For sites at which N_2O production is occurring mainly in the root zone, the production rate per unit thickness of the surface production zone may be found using the van Bavel (1951) equation:

$$P = \frac{2\tau\theta_a D_{AB}\left(C_{deep} - C_{atm}\right)}{a^2} \quad [3]$$

where P is the production rate (M L^{-3} T^{-1}), subscripts A and B represent N_2O and air, C_{deep} and C_{atm} are N_2O concentrations at depth and in the atmosphere (M L^{-3}), and a is the thickness of the surface layer production zone (L). The resulting average flux per unit area, F, is obtained by multiplying Eq. [3] by the production zone thickness:

$$F = \frac{2\tau\theta_a D_{AB}\left(C_{deep} - C_{atm}\right)}{a} \quad [4]$$

For steady-state conditions, determination of N_2O flux using Eq. [4] requires calibration data only for the surface layer, as the average depth profile is unaffected by the transport properties of the lower layers. For sites at which N_2O production can be determined using the above equations, production was still computed using UCODE to provide a measure of the variance in the estimate due to scatter in the concentration data.

Simulation Results

Rangeland Sites

Model simulations for the rangeland sites were, in general, quite straightforward. The sampling nests are located within areally extensive plots of relatively uniform cover, so transport should be well represented by a one-dimensional model. Water levels at two of the sites have remained essentially constant with time, but have declined by about 2.5 m since the 1970s at the NHP rangeland site, presumably due to regional irrigation development. All sites were simulated as having a constant water table. Moreover, the sites have not been subject to a change in land use in historical times, so the effects of unknown initial conditions for the N_2O profile, set to 310 nm^3 m^{-3} at all sites for a start date of 1940, do not affect the results of the 60-yr simulations.

Central High Plains Rangeland Site

Gas samples collected for CFC-12, CFC-11, and SF_6 at the Central High Plains rangeland site (CNG) in August 2001 were used in calibration of a six-layer model. Depth intervals, total and drained porosities, and Millington-computed and UCODE-derived tortuosities are shown in Table 2, and the resulting fit of simulated (lines) to measured (symbols) normalized concentrations are shown in Fig. 5A. The CFC-113 data from shallow depths showed consistently elevated concentrations relative to Niwot Ridge atmospheric data, and were not used in the calibration, but the simulated results are shown. The CFC and SF_6 concentrations at this site showed more scatter among the various CFC and SF_6 data than was observed at most other sites for

TABLE 2. Summary of layer properties and UCODE-based calibration estimates of layer tortuosities for six High Plains sites.

Depth interval	Total porosity	Drained porosity	Millington τ†	τ, UCODE (σ)	CV	Lithology
m						
Central High Plains rangeland site (CNG)						
0.0–9.5	0.38	0.30	0.42	0.31 (0.11)	0.35	Very fine to coarse sand, silty
9.5–17	0.38	0.21	0.18	0.14 (0.034)	0.25	Very fine sand to silty gravel
17–23	0.38	0.325	0.50	0.35 (0.48)	1.4	Fine to coarse sand and gravel
23–34	0.34	0.17	0.14	0.13 (0.025)	0.20	Fine sand with silt, clay and gravel
34–43	0.38	0.31	0.45	0.083 (0.048)	0.58	Fine sand, silty, to coarse sand
43.5–50	0.43	0.04	0.0030	0.0030 (fixed)	NA	Sand, clayey silty
Northern High Plains rangeland site (IMP)						
0–5	0.38	0.27	0.33	0.16 (0.08)	0.47	Sand, very little silt
5–13	0.37	0.12	0.052	0.15 (0.027)	0.19	Very silty sand, clay, gravel
13–27.5	0.39	0.17	0.10	0.058 (0.0064)	0.11	Silty sand, some clay, to gravel
Northern High Plains irrigated corn site at Yuma (UMA)						
0–8	0.325	0.13	0.081	0.16 (0.018)	0.11	Sand, clayey, silty
8–12	0.35	0.18	0.15	0.026 (0.0022)	0.083	Sand, silty, clayey, gravel
12–35	0.33	0.20	0.21	0.23 (0.045)	0.19	Medium sand, silty
35–47.5	0.36	0.17	0.12	0.063 (0.024)	0.38	Sand, silty, clayey, gravel
Northern High Plains irrigated corn site at Grant (GNT)						
0–11	0.35	0.15	0.098	0.16 (0.024)	0.15	Silty sand, clayey
11–17	0.35	0.25	0.32	0.52 (2.2)	4.2	Sand and gravel
17–34	0.35	0.15	0.098	0.036 (0.0050)	0.14	Silty sand, some gravel
34–45	0.35	0.13	0.070	0.0042 (0.0022)	0.54	Clay, sand, and silt, gravelly
Central High Plains Conservation Reserve Program site (CAL-121)						
0–20	0.40	0.20	0.15	0.25 (0.016)	0.13	Very silty fine to medium sand
20–45	0.30	0.23	0.36	0.13 (0.028)	0.25	Medium to coarse sand, gravel
Southern High Plains irrigated cotton site at Cochran County (JRW)						
0–46	0.37	0.24	0.26	0.22 (0.0061)	0.027	Silty sand to gravel
Southern High Plains irrigated cotton site at Maple (MPL)						
0–14	0.34	0.16	0.12	0.37 (0.055)	0.15	Very silty sand, some clay
14–20	0.34	0.15	0.10	0.16 (0.036)	0.23	Sand, gravel
20–42	0.36	0.23	0.25	0.063 (0.0027)	0.044	Sand, some gravel

† Millington tortuosity.

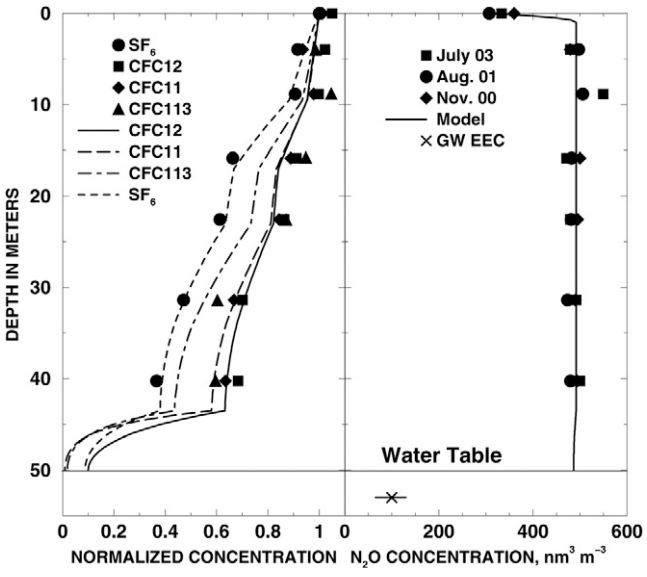

FIG. 5. (A) Chlorofluorocarbon and SF_6 concentrations measured in August 2001 samples from the Central High Plains rangeland site CNG (symbols) compared with simulated profiles (lines) for porosity, moisture content, and tortuosity data shown in Table 2; and (B) measured N_2O profiles compared with the simulated profile assuming that steady 0.17 kg N_2O-N ha^{-1} yr^{-1} production occurs in the top 1 m of the profile. X in line represents mean and range of groundwater equivalent equilibrium concentration in water-vapor-saturated air (GW EEC).

this study, for unknown reasons, but a reasonably good fit was obtained.

Nitrous oxide production was estimated using N_2O profiles for November 2000, August 2001, and July 2003 (Fig. 5B). The profiles indicate a nearly uniform concentration of about 490 nm^3 m^{-3} below a depth of about 15 m. Assuming a mean atmospheric N_2O concentration of 310 nm^3 m^{-3}, drained porosity of 0.30, a τ of 0.31 ± 0.11 for the surface layer (Table 2), a free-air N_2O diffusion coefficient of 1.36 m^2 d^{-1} under prevailing site conditions, and a production interval of 1 m, Eq. [4] indicates an average N_2O flux of 46 ± 16 nm^3 m^{-3} m^{-2} d^{-1} or 0.17 ± 0.065 kg N_2O-N ha^{-1} yr^{-1} (Table 3), where the uncertainty is due to that in the τ determination for the top layer. A simulation using UCODE, made to provide a statistical fit to the profile, yielded a production rate of 45.4 ± 1 nm^3 m^{-3} m^{-2} d^{-1}. For the UCODE analysis, no uncertainty is assigned to tortuosity, so the indicated σ is due only to N_2O data scatter.

The NO_3^- profile at this site provides inconclusive evidence of denitrification as a source of N_2O. The NO_3^- concentration is below the detection limit of 0.05 mg N kg^{-1} sediment in the top 2 m, but reaches a level of 259 mg N kg^{-1} sediment at a depth of 3.2 m, presumably due to evaporative enrichment (McMahon et al., 2003, p. 27). Walvoord et al. (2003) analyzed NO_3^- evaporative enrichment as related to the concentration peak at this and other sites in arid and semiarid environments in detail.

Northern High Plains Rangeland Site

The CFC and SF_6 data for August 2003 were used for model calibration at the Northern High Plains rangeland site (IMP). The vadose zone was divided into three layers for calibration, including a surface sandy layer and two silty sand layers that each incorporated a thin sandy layer. Layer properties and the resultant fit of the simulations to the CFC data are listed in Table 2 and shown in Fig. 6A.

Nitrous oxide production was estimated from N_2O data collected in February, May, and August 2003. The N_2O concentrations are nearly uniform at depth, with shallow profiles typical of those showing seasonal root-zone production. The increase in concentration at depth indicates a mean flux, assuming a 1-m production interval, of about 0.04 ± 0.02 kg N_2O-N ha^{-1} yr^{-1} for τ = 0.16 ± 0.08 for the top layer. The measured shallow profiles are matched reasonably well by assuming that the entire flux occurs as a seasonal pulse lasting from 15 April until 25 August (Fig. 6B). This pattern is consistent with the noted dependence of the rate of denitrification and N_2O production on increasing temperature and on soil moisture content (Parton et al., 1996). Soil temperature increases during the spring and summer months, but begins to decline from its snow-melt- and spring-rain-generated maximum by late spring.

TABLE 3. Summary of N_2O fluxes, N application rates, soil water and groundwater NO_3 concentrations, and groundwater N_2O concentrations for seven High Plains sites.

Site ID	Location†	Cover	Nitrogen applied	One-dimensional model estimates of N_2O production			NO_3 concentration (avg. N_2O EEC‡ in groundwater)		
				Root zone	Deep unsaturated zone	Water table	Root zone	Deep unsaturated zone	Groundwater
			kg ha^{-1} yr^{-1}	kg N_2O-N ha^{-1} yr^{-1}			mg N kg^{-1} soil		mg N L^{-1} (nm^3 m^{-3})
CNG	Kansas (CHP)	range	6.6§	0.17 ± 0.065	0.0	0.0	<0.1	259 (2–10 m)	1.2 (110)
IMP	Nebraska (NHP)	range	6.8	0.04 ± 0.02	0.0	0.0	2.0	<0.1	2.8 (325)
MWR	Texas (SHP)	range	4.2	<0.01	0.0	0.0	2.7	<0.1	0.2 (NA¶)
UMA	Colorado (NHP)	corn	250#	2.3 ± 0.3	0.0	0.0	31	2 (32–38 m)	2.0 (424)
GNT	Nebraska (NHP)	corn	225	1.3 ± 0.25	0.0	0.0	10	6 (10 m) 10.5 (20 m) 3 (22–43 m)	8.5 (1565)
CAL-121	Kansas (CHP)	grass	225	<0.01	0.023 ± 0.004†† 0.017 ± 0.004‡‡	0.016 ± 0.003†† 0.004 ± 0.003‡‡	<1	15 (15–17 m) 5 (35 m)	23 (1355)
JRW	Texas (SHP)	cotton	300	0.074 ± 0.033	0.0	0.009 ± 0.0006	4	2.9 (15 m) 2.8 (30 m)	3.8 (1160)

† SHP, Southern High Plains; CHP, Central High Plains; NHP, Northern High Plains.
‡ Equivalent equilibrium concentration in water-vapor-saturated air.
§ Rangeland rates assumed to equal two times the total inorganic N concentration in wet deposition (see McMahon et al., 2006).
¶ NA = not available.
# Producer records show increasing fertilizer use with time. All irrigated site data represent recent (1990+) application rates. For the CHP sites, the application is to the nearby corn fields.
†† Initial profile of 310 nm^3 m^{-3} assumed.
‡‡ Initial profile of 4000 nm^3 m^{-3} assumed.

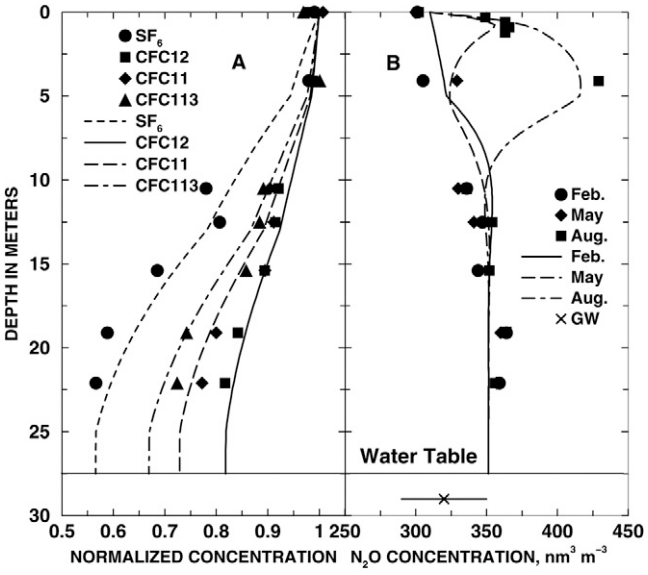

FIG. 6. (A) Chlorofluorocarbon and SF_6 concentrations measured in August 2003 samples from the Northern High Plains rangeland site IMP (symbols) compared with simulated profiles (lines) for porosity, moisture content, and tortuosity data shown in Table 2; and (B) match of simulated (lines) seasonally distributed root-zone N_2O production of 0.04 kg N_2O-N ha^{-1} yr^{-1} to measured concentrations. X in line represents mean and range of groundwater (GW) equivalent equilibrium concentration in water-vapor-saturated air.

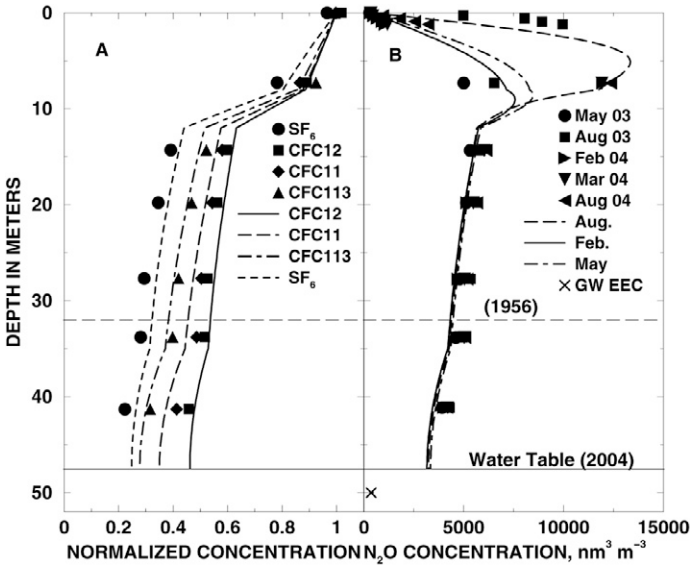

FIG. 7. (A) Chlorofluorocarbon and SF_6 concentrations at the Northern High Plains irrigated corn site UMA measured in May 2003 compared with simulated profiles for porosity, moisture content, and tortuosity data shown in Table 2; and (B) comparison of simulated to measured N_2O concentrations for root-zone production of 2.3 kg N_2O-N ha^{-1} yr^{-1} occurring seasonally. X in line represents mean and range of groundwater equivalent equilibrium concentration in water-vapor-saturated air (GW EEC).

Southern High Plains Rangeland Site

Nitrous oxide production at the Southern High Plains rangeland site (MWR) appears to be minimal, based on N_2O concentrations at depth (not shown) that are about equal to those in the atmosphere, despite the fact that high soil-moisture NO_3^- concentration, a common correlate to N_2O production zones, occurred in the shallow subsurface at this site (Fig. 2). Based on these observations, no calibration was made, and N_2O production was assigned a value of below detection limit (about 0.01 kg N_2O-N ha^{-1} yr^{-1} for root-zone production).

Irrigated Sites

Simulation results for the irrigated sites are seriously affected by edge effects resulting from placement of the sampling nests at the edge of the irrigated fields. Based on the deep N_2O profiles collected during this study, as well as the results of numerous other studies, as summarized for native vegetation by Bowden (1986) and for fertilized crops by Eichner (1990), N_2O production is substantially greater from the irrigated and fertilized fields than from the adjacent rangeland. The contrasting adjacent production rates result in an edge effect that is not accounted for by the one-dimensional model. A preliminary two-dimensional model investigation using fictitious parameters that mimic those governing diffusive gas transport in a uniform medium in the code VS2DT (Healy, 1990) indicates that equilibration at depth at the edge of root-zone production adjoining an area with no root-zone production is substantially delayed relative to that simulated using a one-dimensional model, and that the production rate based on the use of a one-dimensional model would be underestimated by a factor of about 2. Ideally, these edge effects should be investigated using a two-dimensional model. For this study, however, the potential effects are only acknowledged and the potential effects estimated using this factor of 2 uncertainty.

A second complication affecting the simulations for the irrigated sites, particularly those for which a change in land use or irrigation practice occurred with 15 yr or so of N_2O sampling, arises from uncertainty in the initial conditions assumed for the start of the simulation period. The impact of that uncertainty on the possible range of N_2O production rates was tested by sensitivity analysis, as described individually for these sites.

Significant declines in water table elevation, beginning with the onset of irrigation, were observed at each of the irrigated sites. These declines were simulated as occurring at a uniform rate beginning near the onset of irrigation, using the annual rate of decline for each site listed in Table 1.

Northern High Plains Yuma Irrigated Site

The Northern High Plains irrigated site at Yuma, CO, (UMA) has been planted to irrigated corn since 1956, with flood irrigation through 1988 and center-pivot sprinkler irrigation afterward. The model for this site was calibrated using CFC and SF_6 data obtained in May 2003. The 47.5-m-thick vadose zone was divided into four layers, as listed in Table 2. Calibration results for the 8- to 12-m layer provide a much lower τ than is provided by the Millington equation. Presumably a thin, tight zone not detected in drill cuttings occurs in that layer. Calibration resulted in CFC-12 and SF_6 concentrations being overpredicted, and those for CFC-11 and CFC-113 being underpredicted, as shown in Fig. 7A.

Nitrous oxide production was simulated using N_2O profile data (Fig. 7B) from measurements in May and August 2003, and February, March, and August 2004. The profiles for the last four sampling events include data from four shallow probes extending from the land surface to a depth of 1.2 m in 0.3-m increments. These data demonstrate the occurrence of strongly seasonal N_2O production in the root zone that has not occurred

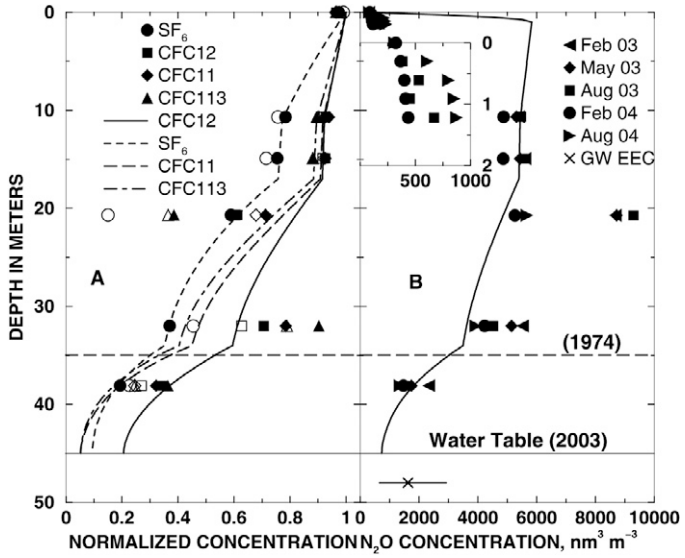

FIG. 8. (A) Chlorofluorocarbon and SF6 concentrations at the Northern High Plains irrigated corn site GNT measured in May (filled symbols) and August 2003 (open symbols) compared with simulated profiles for porosity, moisture content, and tortuosity data shown in Table 2; and (B) comparison of simulated (solid line) to measured N_2O concentrations for steady root-zone production of 1.3 kg N_2O-N ha^{-1} yr^{-1}. Inset shows mismatch between shallow and deep data. X in line represents mean and range of groundwater equivalent equilibrium concentration in water-vapor-saturated air (GW EEC).

for a sufficient time for concentrations at depth to equilibrate with that production. The presence of root-zone production, but none at depth, is supported by the soil-moisture NO_3^- profile (Fig. 2), which indicates quite high NO_3^- in the near surface, but very low concentrations below the soil zone. Simulations using the one-dimensional model with UCODE indicate that average root-zone production of 2.3 ± 0.3 kg N_2O-N ha^{-1} yr^{-1} in a 1-m-thick zone for a specified period of 18 yr provides an excellent fit to the deeper data (Fig. 7B). The shallow data are somewhat well matched if the production is assumed to occur as a rectified sine wave beginning 15 April and lasting until 15 June, with results splitting the differences between measured profiles for August 2003 and August 2004.

Trial and error simulations of root-zone production for the full 47 yr of irrigation (not shown) provided a nearly uniform concentration below a depth of about 15 m, thus failing to match the measured profiles and precluding the use of UCODE to determine a N_2O flux for that full period. The known history of fertilizer applications at this site starts in 1986, with the tenure of the current owner, but similar fertilizer applications presumably date back to the advent of irrigation in 1956. The lack of equilibration of N_2O concentrations at depth during this 47-yr period probably results from an edge effect due to the location of the sampling nest just outside the irrigated field, as described above. Based on the indication that edge effects would cause the production rate computed using a one-dimensional model to be underestimated by a factor of about 2, N_2O production within the irrigated field at the UMA site may be approximately 4 to 6 kg N_2O-N ha^{-1} yr^{-1}.

Northern High Plains Grant Irrigated Site

The Northern High Plains irrigated site at Grant, NB, (GNT) has been planted to sprinkler-irrigated corn since 1974. The CFC and SF_6 data are available for May and August 2003, but the May CFC data show some residual effects of drilling air, and data for two probe levels (21 and 32 m) are quite inconsistent, in relation both to their depths and to sampling dates, for unexplained reasons. Concentrations of all species for the 21-m depth and those for CFC-11 and CFC-113 at the 32-m depth were not used for model calibration. For calibration, the vadose zone was divided into four layers, as listed in Table 2. Results (Fig. 8A) indicate an excellent fit to all data for the 10.7- and 14.9-m depths, and surprisingly low τ values for the deeper layers, possibly due to unrecognized layering by interbedded fine-grained materials.

Nitrous oxide production was estimated using N_2O data for February, May, and August 2003, and February and August 2004, and additional data from four shallow probes for the latter three dates. A complication for analyzing the N_2O data for this site is that the shallow-probe data do not match the deep data, instead showing a parabolic shape indicative of much lower seasonal production in a thin shallow zone (Fig. 8B). A possible cause of this mismatch is that a nearly impervious (to gas transport) laterally discontinuous layer below the shallow nest (>1.2 m) separates the surface probes from the shallowest (11-m) deep probe, and the deep profile is responding to N_2O production in the adjacent corn field. A second complication arises from the extremely high, and highly variable, N_2O concentration in the 21-m probe. Attempts to model this concentration as a temporary source returning to a production rate of 0 were not successful.

The shallow profiles and the aberrant concentrations in the 21-m probe were ignored for the model N_2O production estimate. Based on the τ values listed in Table 2, a UCODE fit, assuming production started with the advent of irrigation in 1974, provides steady root-zone production of 1.3 ± 0.25 kg N_2O-N ha^{-1} yr^{-1}. Edge effects for the one-dimensional model probably result in an underestimate by a factor of about 2, so production could be about 2 to 3 kg N_2O-N ha^{-1} yr^{-1}.

Central High Plains Irrigated Sites

Quantification of N_2O production using data collected at the two CHP sites, both associated with irrigated corn, is complicated by the site locations and changes in agricultural practice. The instrumented sites at both locations were installed about 75 m from the edge of the irrigated crop within the triangular area that had been flood-irrigated from 1955 and 1956, but is not reached by center-pivot irrigation, initiated in 1990. These areas are now planted to grass as part of the Conservation Reserve Program. Thus, these sites received fertilizer and irrigation water from about 1956 to 1990, but were not irrigated or fertilized thereafter. During the 30+ year period that the sampling sites had been flood-irrigated and planted to corn, the N_2O profile probably became similar, within a range of considerable uncertainty, to those measured adjacent to currently irrigated corn at the UMA and GNT sites, and thus quite elevated. Model sensitivity analysis, based on a range of plausible estimates for N_2O initial conditions, was used to estimate a range of production rates at the Central High Plains Agricultural Land Use Study site CAL-121, but this approach did not appear feasible for site CAL-122, which is not further discussed.

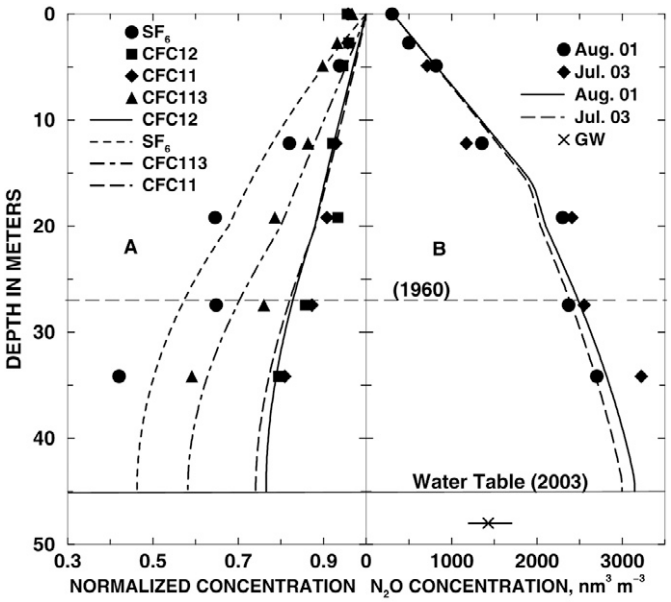

FIG. 9. (A) Chlorofluorocarbon and SF_6 concentrations at the Central High Plains Conservation Reserve site CAL-121 measured in August 2001 compared with simulated profiles for porosity, moisture content, and tortuosity data shown in Table 2; and (B) comparison of simulated to measured N_2O concentrations for production of 0.017 kg N_2O-N ha^{-1} yr^{-1} at the 15- to 17-m zone and 0.004 kg N_2O-N ha^{-1} yr^{-1} at the water table, beginning in 1990 with an initial concentration of 4000 nm^3 m^{-3}. X in line represents mean and range of groundwater (GW) equivalent equilibrium concentration in water-vapor-saturated air.

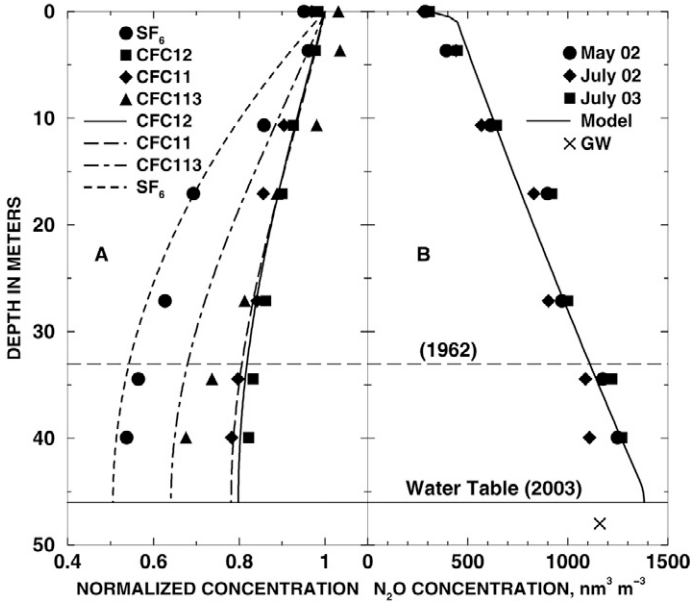

FIG. 10. (A) Chlorofluorocarbon and SF_6 concentrations measured in July 2002 at the Southern High Plains irrigated cotton site JRW compared with simulated profiles for porosity, moisture content, and tortuosity data shown in Table 2; and (B) comparison of simulated to measured N_2O concentrations for root-zone production of 0.074 kg N_2O-N ha^{-1} yr^{-1} and water table production of 0.009 kg N_2O-N ha^{-1} yr^{-1}. X is a single measurement of groundwater (GW) equivalent equilibrium concentration in water-vapor-saturated air.

The CFC and SF_6 data for August 2001 (Fig. 9A) were used in model calibration for the CAL-121 site. The 45-m-thick vadose zone was divided into two layers. Final results, based on matching CFC-11, CFC-12, and SF_6 data, are summarized in Table 2.

Nitrous oxide production was evaluated based on N_2O profiles obtained in August 2001 and July 2003 (Fig. 6B). Zones of N_2O production were inferred from the soil-water NO_3^- distribution with depth (Fig. 2), which shows almost no NO_3^- in the soil zone, a strong NO_3^- peak at a depth of about 15 m, and an elevated NO_3^- concentration in the groundwater. Examination of the N_2O profiles indicate the possibility that all data but the 34-m depth reading for July 2003 either might be explained by production at the 15-m depth and at the water table, or may reflect only the residual effects of previous N_2O production during corn cultivation. Three sets of initial conditions were evaluated, including uniform profiles of 310, 4000, and 8000 nm^3 m^{-3}, computed assuming previous production rates of 0, 2, and 5 kg N_2O-N ha^{-1} yr^{-1} for a period of 30 yr. All simulations started at the beginning of 1990. Results for initial profiles of 310 and 4000 nm^3 m^{-3} provided plausible results, but an initial concentration of 8000 nm^3 m^{-3} required consumption at the water table about equal to production at the 15- to 17-m level, values that are physically implausible. Results for the initial profile of 310 nm^3 m^{-3} indicate production of 0.023 ± 0.004 and 0.016 ± 0.003 kg N_2O-N ha^{-1} yr^{-1} from the 15- to 17-m zone and from the water table, respectively, while for an initial profile of 4000 nm^3 m^{-3}, production is 0.017 ± 0.004 kg N_2O-N ha^{-1} yr^{-1} in the 15- to 17-m zone and 0.007 ± 0.003 kg N_2O-N ha^{-1} yr^{-1} from the water table. Simulated results are shown (Fig. 9B) for an initial concentration of 4000 nm^3 m^{-3}.

Southern High Plains Cochran County Irrigated Cotton Site

Model calibration for the Southern High Plains irrigated cotton site at Cochran County, TX, (JRW) was based on CFC data collected in July 2002. The 46-m vadose zone was initially divided into six layers, but UCODE results indicated that the vadose zone can be analyzed as a single layer. The one-layer simulation provided a quite satisfactory fit to data for CFC-12, CFC-11, and SF_6 collected in August 2001 (Fig. 10A), based on a τ of 0.22 ± 0.006 (Table 2). The near-surface CFC-113 concentrations exceed those in the Niwot Ridge atmospheric record by a few percentage points, and were not included in the automatic fitting routine.

Nitrous oxide production was estimated from N_2O data for May and July 2002 and July 2003. The N_2O profiles show a small offset to higher N_2O concentration at shallow depth and a nearly uniform slope toward a maximum concentration near the water table, indicative of production at the water table. A comparison of these zones to the soil-moisture NO_3^- profile (Fig. 2) shows a high near-surface concentration, secondary peaks at depths of about 15 and 30 m, and NO_3^- concentration of 0.75 mg kg^{-1} sediment (3.8 mg L^{-1}) in groundwater at the water table. The source of N_2O at depth may arise from denitrification of groundwater, with its release to soil gas being enhanced by the declining water table.

Uncertainty regarding the initial N_2O profile exists as a result of the site being within the irrigated field until 1990, and on its edge thereafter. The time at which production of N_2O

at the water table began is also uncertain, but undoubtedly followed the start of irrigation, as the presumed groundwater NO_3^- source probably migrated from the land surface as irrigation return flow. A sensitivity analysis was made by conducting a series of simulations for uniform initial concentrations in 1990 ranging from 310 to 900 $nm^3\ m^{-3}$, and one simulation based on a non-uniform initial profile created by simulating root-zone production of 40 $nm^3\ m^{-3}\ m^{-2}\ d^{-1}$ and water-table production of 2 $nm^3\ m^{-3}\ m^{-2}\ d^{-1}$ lasting from 1970 to 1990. The results of these one-dimensional simulations indicate that gas-phase transport is rapid enough at this site that initial conditions as of 1990 are not significant and can be ignored. Production of 0.074 ± 0.033 kg N_2O-N $ha^{-1}\ yr^{-1}$ in the 1-m root zone and 0.009 ± 0.0006 kg N_2O-N $ha^{-1}\ yr^{-1}$ in a 2-m interval immediately above and following the water table provides a good match to the measured profiles, as shown in Fig. 10B. Estimated root-zone production is compromised by crop edge effects, but production from the water table may represent an areally extensive effect, and hence should be reliable.

Southern High Plains Maple Irrigated Cotton Site

The CFC and SF_6 data from the Southern High Plains irrigated cotton site at Maple, TX, (MPL) for July 2002 provided an excellent calibration fit (not shown) for all four species, using a three-layer model. Results of the calibration are listed in Table 2, as they add to the catalog of field-based tortuosities for diffusive transport investigations. The N_2O measurements, however, available for dates in September 2001, and February, May, and July 2002, show a great deal of scatter, particularly those for depths >10 m, and simulation results for the site are very sensitive to initial conditions assumed for 1990. This sensitivity, combined with the large scatter in the data, provided inconclusive results as to whether the N_2O profiles resulted from N_2O production in selected zones or were only a residual effect of prior conditions.

Results and Discussion

Model Calibration

Calibration results for the seven sites for which it was feasible are listed in Table 2, including depth intervals of chosen layers, arithmetically averaged total and air-filled porosities, Millington τ value, and the UCODE-determined mean value, σ (standard deviation), and CV of the tortuosity for each layer. A variety of additional statistics regarding the reliability of the calibrations are provided by UCODE (Hill, 1998; Poeter and Hill, 1998). Twelve of the 22 layers for which calibration data are available provided τ values with CVs of 0.2 or less, and all but four had CVs <0.5. These four include two for the GNT Northern High Plains irrigated corn site, for which the CFC data were subject to substantial uncertainty due to unknown processes, and two for the CNG Central High Plains rangeland site, for which the CFC data showed substantial scatter among layers. Also, the two determinations of CV >1 are for layers that exhibited small concentration gradients, resulting in large, but insensitive, τ values. The exact magnitude of the τ values for these layers is not known, but use of the indicated values or others of similar magnitude will have little effect on the reliability of predictions of gas transport. Overall, the fit between measured and simulated concentrations for the four species is quite good (Fig. 5–10), and the calibrated models should be quite adequate to simulate the one-dimensional transport of other trace gas species.

The UCODE-based τ values show poor agreement with those computed using the Millington equation (Table 2), with the mean of the UCODE values being about 15% smaller than that for the Millington values, due in large part to the results of eight layers for which the UCODE-derived values are less than half the Millington values. This lack of agreement may arise from the inadequacy of representing the porosity and moisture content of layers of somewhat heterogeneous sediments, ranging in thickness from 4 to 46 m, with values derived from the four to six cores collected at each site. In particular, the use of cores and drill cuttings to characterize the full thickness of the vadose zone may fail to identify thin layers of finer grained or more tightly cemented materials. Such layers may greatly restrict gas-phase diffusive transport, but be unaccounted for during estimation of total and air-filled porosity. Moreover, considerable uncertainty exists in estimating an appropriate Millington τ for a heterogeneous layer, even with perfect knowledge of the variations in total and air-filled porosity. Due to the strong nonlinearity of the Millington τ (Eq. [2]) with respect to both total and air-filled porosity, use of thickness-weighted arithmetic average values for those parameters would result in an overestimate of the effective τ value in moderately heterogeneous media. Thus, as suggested by Werner et al. (2004), a field method, such as the one used here, is needed to identify effective gas-phase diffusivity in many situations.

The assumption that CFC concentrations measured at Niwot Ridge, CO, adequately represents that at rural sites in general has been widely made (Busenberg et al., 1993; Severinghaus et al., 1997; Engesgaard et al., 2004). This assumption appears adequate for this study as well, based on a comparison of measured atmospheric values to those interpolated from the Niwot Ridge tabulation. The mean ratio of measured to interpolated concentrations for the different species ranged from 0.98 to 1.00 (excluding results for one anomalous CFC-12 sample from the CAL-122 site that was 160% of the Niwot Ridge record), with standard deviations ranging from 0.017 to 0.044.

Simultaneous measurements of all four gas species (except as noted in Table 2) were used for calibration, based on the assumption that none of the species are being degraded or sorbed to the solid phase. The CFCs are noted to be biodegraded in anaerobic but not in aerobic environments (Busenberg and Plummer, 1992, p. 2266), and, as the vadose zone overlying the High Plains aquifer is well oxygenated, degradation of CFCs is unlikely. Assumptions regarding sorption are more problematic. Weeks et al. (1982) assumed sorptive behavior in calibrating a diffusion model to CFC-11 and CFC-12 measurements at other sites in the SHP, based on the work of Brown (1980). Severinghaus et al. (1997) matched CFC profiles measured in large sand dunes using a similar diffusion model while ignoring sorption, and Engesgaard et al. (2004) found that sorption of CFC-11 was minor at a sandy site in Denmark. Santella et al. (2006) estimated K_s (water–solid distribution coefficient) values of 0.0, 0.02, and 0.1 for CFC-12, CFC-11, and CFC-113, respectively, as part of a detailed study at a site near Sparkill, NY. From Eq. [2], these distribution coefficients, assuming average site conditions, would result in 7 and 10% decreases in

the effective diffusion coefficients for CFC-11 and CFC-113, respectively, relative to the values computed assuming no sorption. Graphical comparisons of simulated to measured values for the four species, however, indicate no systematic tendency for CFC-11 or CFC-113 concentrations to be overestimated relative to those for CFC-12 and SF_6, indicating that, within the accuracy of the available data, sorption of CFCs can be ignored in this study.

Nitrous Oxide Production

Estimates of N_2O production (Table 3) were obtained for rangeland at three sites, two corn fields in the NHP, one Conservation Reserve Program ungrazed grassland site previously planted to corn in the CHP, and one cotton field in the SHP. Our technique allows determination of both magnitude and depth location of N_2O production, including within the root zone, at depth in the vadose zone, and at the water table. Detectable root zone production was determined for five sites, in the deep vadose zone for one site, and from groundwater at two sites. Most zones of measurable N_2O production are associated with higher NO_3^- in soil water or in groundwater near the water table, but not all zones of higher NO_3^- are associated with N_2O production (Fig. 2, Table 3). Root-zone production is generally the major source of N_2O, but its estimation is subject to greater uncertainty than those for production at depth.

Root-Zone Production

Nitrous oxide production at the three rangeland sites ranges from about 0.2 kg N_2O-N ha^{-1} yr^{-1} at the CHP rangeland site (CNG; Table 3) to <0.01 kg N_2O-N ha^{-1} yr^{-1} at the SHP rangeland site (MWR). Modest N_2O production of 0.04 kg N_2O-N ha^{-1} yr^{-1} occurs at the NHP rangeland site (IMP), compared with the MWR site, despite the fact that its root-zone NO_3^- concentration (Fig. 2) is slightly less. This contrast may result from the fact that the MWR site is sandier (better drained) and drier than the other rangeland sites, as N_2O production varies with soil moisture content (Parton et al., 1996). The production estimate for the CNG site agrees well with the 3-yr average production rate of 0.17 kg N_2O-N ha^{-1} yr^{-1} for unfertilized native pasture in eastern Colorado listed by Mosier et al. (1997, p. 39), and with a value of 0.2 kg N_2O-N ha^{-1} yr^{-1} determined for Wisconsin prairie by Goodroad and Keeney (1984). Nitrous oxide production at the other rangeland sites is lower than most reported values for similar vegetative cover.

Nitrous oxide data from both sites planted to irrigated corn in the NHP indicate substantial root-zone N_2O production. The one-dimensional model estimates indicate production rates of about 2 to 6 kg N_2O-N ha^{-1} yr^{-1}, as adjusted for edge effects. Estimates of N_2O flux from the corn fields are similar to those reported in the literature, including, among others, values of 3.6 and 5.2 kg N_2O-N ha^{-1} yr^{-1} determined from corn fields in Wisconsin (Eichner, 1990, Table 2), and of 4.2 kg N_2O-N ha^{-1} yr^{-1} from a no-till corn field in Tennessee (Thornton and Valente, 1996, p. 1127).

Root-zone production at the CHP irrigated CAL-121 site is indicated to be <0.01 kg N_2O-N ha^{-1} yr^{-1}, but could not be reliably estimated for the CAL-122 site. Comparison of N_2O production rates for the CAL-121 site to those for irrigated corn sites in the NHP indicate that conversion from corn cultivation to Conservation Reserve Program status may have significantly reduced N_2O production. Assuming that N_2O production in the soil zones of the corn fields adjacent to the Conservation Reserve Program sites is similar to that from the NHP sites, our results indicate that the cropland conversion may have decreased the production rate by a factor of 10 or more.

The N_2O profiles for the SHP irrigated cotton site JRW indicate root-zone production of about 0.15 kg N_2O-N ha^{-1} yr^{-1}, based on a factor of 2 impact of edge effects on the one-dimensional model estimate. The estimate is significantly smaller than the loss rate of 2 kg N_2O-N ha^{-1} yr^{-1} determined for a flood-irrigated cotton crop planted in clay soil in Australia (Rochester, 2001, p. 197). The SHP cotton fields are sandy, and are irrigated by sprinkler. The different results from those of Rochester (2001) may reflect the effects of soil texture or of water application mode (or both) in N_2O generation, or may be due to uncertainties involved in the use of the proposed technique.

Estimates for root-zone production are quite uncertain, for reasons in addition to those regarding edge effects and initial conditions that apply circumstantially to different sites. A major uncertainty is that involving the true depth of root-zone production. From Eq. [4], N_2O production for a given concentration at depth is inversely proportional to root-zone thickness, which we assume to be 1.0 m. The active layer of N_2O production may extend from the land surface to a shallower depth, say 0.5 or 0.3 m, resulting in a bias toward too-small fluxes by a factor of 2 or 3. Uncertainty also arises from the use of a τ value for a composite surface layer of a few to several meters thickness (Table 2) to represent that for the thin soil zone. The soil-zone effective τ is probably larger than that for the composite layer because of effects of barometric pumping (Massmann and Farrier, 1992), and possibly due to the presence of dessication cracks, root holes, and animal burrows. Santella et al. (2003, p. 1073), however, made very detailed SF_6 measurements in the shallow subsurface at a site near New York City, which they successfully simulated using an estimated τ of 0.19, a value that agrees well with the surface layer τ values of 0.24 ± 0.08 determined for this study. This result suggests that soil-zone τ values may, in fact, be similar to those determined for thicker surface layers, and that uncertainty of production estimates due to this source may be minor.

Production from Below the Root Zone

Long-term slow rates of N_2O production were indicated within the vadose zone or at the water table at the CAL-121 and JRW sites (Table 3). For the CAL-121 site, a sensitivity analysis involving various assumed initial N_2O profiles indicates a probable production rate from a zone of elevated soil-moisture NO_3^- at a depth of about 15 m of about 0.01 to 0.02 kg N_2O-N ha^{-1} yr^{-1}, and production from the water table of about 0.004 to 0.016 kg N_2O-N ha^{-1} yr^{-1}. Groundwater at the site has a higher NO_3^- content (4.5 mg NO_3^-–N kg^{-1} sediment or 23 mg N L^{-1}) than at other sites. For the JRW site, indicated production from the water table is about 0.009 kg N_2O-N ha^{-1} yr^{-1}. Groundwater at the site has a NO_3^- concentration of 3.8 mg NO_3^-–N kg^{-1} sediment.

Estimates of production at depth are based on the assumptions that the source layer, either a zone of high NO_3^- content within the vadose zone or high-NO_3^- groundwater, is areally

extensive, and that the production has been occurring since the start of irrigation or the last change in land use, or for sufficient time to avoid the effects of assumed initial conditions, a period of at least several years. The estimates are subject to fewer uncertainties than those for root-zone production because the concentration gradients generated by even very small N_2O fluxes at depth are large enough to be accurately determined, and values for effective diffusion coefficients at depth are better constrained by the CFC data than are those for the soil zone.

Simultaneous measurement of N_2O concentrations in groundwater at the various sites (Table 3) provide insight into possible mechanisms of N_2O production and consumption. The groundwater NO_3^- EEC (Fig. 5–10, Table 3) are lower or about equal to those in the deep vadose zone at each site, indicating that the source of N_2O production is within the vadose zone or very near the water table, rather than from a depth of even a few meters in the groundwater reservoir.

The average groundwater N_2O EEC of about 110 nm^3 m^{-3} at the CHP rangeland site CNG (Fig. 5B) is of particular interest, as it is much lower than that in the overlying vadose zone or in the atmosphere, thus suggesting the occurrence of consumption of N_2O in soil water near or just below the water table. Soil-derived N_2O is often produced as an intermediate product by anaerobic denitrification of NO_3^- to N_2, with the N_2O diffusing from soil water into the gas phase, the "hole in the pipe" process described by Firestone and Davidson (1989). Thus, under most conditions, the vadose zone is a source of N_2O to the atmosphere or to the water table. In poorly drained media, however, from which diffusive loss is limited, the rate of denitrification of N_2O to N_2 can exceed that of NO_3^- to N_2O, resulting in depletion of N_2O in soil moisture (Letey et al., 1981; Menyailo and Hungate, 2006). This phenomenon may be occurring in the clayey layer with very high soil moisture content that extends from a depth of 43 to 50 m at the CNG site (Fig. 3). Groundwater containing N_2O at EECs less than atmospheric has also been sampled from shallow wells at localized sites among several showing very high EECs during intensive studies of N_2O flux from poorly drained forested riparian zones (Bowden et al., 1992; Osaka et al., 2006).

Two other studies have made estimates of N_2O production from groundwater. Osaka et al. (2006) combined measurements of N_2O in the shallow groundwater reservoir of a riparian zone with those in the vadose zone, and inferred that groundwater was the source of N_2O land surface flux of about 0.01 to 0.02 kg N_2O-N ha^{-1} yr^{-1}. Ronen et al. (1988, p. 58) estimated N_2O flux from NO_3^-–rich groundwater of 3.4 to 7.8 kg N_2O-N ha^{-1} yr^{-1}, values that may be too high by a factor of 500. A discrepancy between their Fig. 3 axis label units of $\mu g\ L^{-1}$and figure caption units of mg $L^{-1}cm^{-1}$may result in a computed flux value that is too large by a factor of 1000, and their conversion from mass N_2O underestimates mass N_2O-N by a factor of 2. Corrected values result in fluxes from the water table of 0.007 to 0.02 kg N_2O-N ha^{-1} yr^{-1}, in good agreement with the results of our study and those of Osaka et al. (2006). In summary, our estimates of water-table N_2O production of 0.004 to 0.016 kg N_2O-N ha^{-1} yr^{-1} at two of nine sites, combined with the estimates by Osaka et al. (2006) and by Ronen et al. (1988), indicate that denitrification of groundwater is only a minor source of N_2O in the global budget.

Future Work

The method used here to estimate N_2O soil flux should provide a useful tool. Its merits would be greatly enhanced, however, if accompanied by a rigorous program to measure N_2O flux using chambers. In addition to the chamber measurements themselves, measurements of root-zone N_2O, soil moisture, and soil temperature should be made. These measurements, combined with soil-gas concentration modeling at a fine time and space scale, should aid in the interpretation of the chamber measurements. Measured fluxes of N_2O, with its strong dependence on water temperature (Eq. [A2] below), may partially represent the effects of the gas being dissolved or exsolved by cooling or warming soil water. The effect might be particularly relevant during periods of freezing or thawing soil, as Eq. [A2] indicates that storage of N_2O in soil moisture is at a maximum when the soil water is at the freezing point. As the soil freezes, N_2O will be exsolved, and assuming that air-filled pore space remains, will be discharged to the atmosphere. This phenomenon may explain, at least in part, the spikes in N_2O flux measured by Mosier et al. (1997, Fig. 1 and 2) during periods of frozen soil.

Conclusions

Measurements of CFC and SF_6 concentration profiles in an agricultural area underlain by a thick vadose zone have proven useful in evaluating gas-phase transport properties of the unsaturated media. These properties were used with N_2O gas concentration profiles to obtain estimates of flux to the atmosphere of this important greenhouse gas, both from the root zone and from zones at depth in the vadose zone. In several cases, the derived estimates agree well with those determined by other methods. Our methodology provides a means of estimating areally and temporally averaged N_2O fluxes that, although subject to significant uncertainty, should be useful for evaluating soil-zone fluxes to the atmosphere in areas underlain by a thick vadose zone in many settings. Moreover, coupling of such measurements with chamber measurements of N_2O flux would provide information useful for averaging widely varying chamber flux measurements.

Appendix

Properties of Modeled Gases

Gas properties needed to simulate their diffusive transport through the vadose zone include their gas-phase diffusivities and liquid-gas partitioning coefficients. Methodologies used to formulate these data for the three CFCs, SF_6, and N_2O are described below.

Free-Air Gas Diffusion Coefficients

The measured diffusivity for CFC-12 of Monfort and Pellegatta (1991) is in good agreement with that computed using an equation (Bird et al., 1960, Eq. [16.4-13]) based on the Chapman–Enskog kinetic theory. Therefore, that equation has been used to compute diffusivities for the CFC species (Cook and Herczeg, 2000; International Atomic Energy Agency, 2006) and for SF_6 and N_2O here, based on Lennard–Jones parameters for the gases. Perry (1963, Table 14-44) lists Lennard–Jones parameters for CFC-12, but not for CFC-11, CFC-113, or SF_6,

and we are unaware of other published values. Hence, Lennard–Jones parameters for those gases were computed from Bird et al. (1960, Eq. [1.4-11], [1.4-13], [16.4-15], and [16.4-16]). Lennard–Jones parameters for air and N_2O were taken from Bird et al. (1960, Table B1). Diffusion coefficients for a temperature of 0°C and a pressure of 101 kPa for the gases sampled in this study, as well as the relevant parameters used in the computations, are given in Table A1. The diffusivity for N_2O is about 5% smaller than the value given without citation by van Bochove et al. (1998). The tabulated diffusion coefficients are included in a DATA statement in the model, and are corrected for site conditions by dividing by station pressure in atmospheres, and multiplying by the ratio of the mean annual temperature, in K, to 273.16, raised to the 3/2 power.

Solubilities and Air–Water Partitioning Coefficients

The solubilities in water of the gases of interest for this study are governed by Henry's Law of the form (Warner and Weiss, 1985)

$$C = K_T \chi \left(P - P_{H_2O}\right) \quad [A1]$$

where C is the concentration of gas in the liquid phase (mol kg^{-1}); K_T is a temperature-dependent equilibrium constant (mol kg^{-1} atm^{-1}), χ is the mole fraction or partial pressure of the gas in dry air, P is atmospheric pressure (atm); and P_{H_2O} is the water vapor pressure at the prevailing humidity (atm). Values of K_T for distilled water and a given temperature within the range 0 to 40°C may be found from an equation of the form

$$K_T = \exp\left[a_1 + a_2\left(100/T\right) + a_3 \ln\left(T/100\right)\right] \quad [A2]$$

TABLE A1. Properties and free-air diffusion coefficients of modeled gas species.

Gas	T_c†	V_c‡	MW§	$D_{A\text{-}air}$¶
	K	cm^3 mol^{-1}	g	m^2 d^{-1}
Air	NA#	NA	29	NA
SF_6††	318.7	195.8	146.06	0.73
CFC-11‡‡	471	247	137.37	0.62
CFC-12‡‡	385	217	120.91	0.69
CFC-113‡‡	487.3	325	187.4	0.54
N_2O	NA	NA	44.02	1.12

† Critical temperature.
‡ Critical volume.
§ Molecular weight.
¶ Free-air diffusivity of the trace gas species A into air.
# NA = not applicable.
†† Sulfur hexafluoride properties from Mathews (1972).
‡‡ Chlorofluorocarbon properties (except diffusivity) from Weast (1976, p. E34–E35).

TABLE A2. Fitting parameters to compute solubilities in pure water of modeled gas species.

Gas	a_1	a_2	a_3	Reference
CFC-11	–136.2685	206.1150	57.2805	Warner and Weiss (1985)
CFC-12	–124.4395	185.4299	51.6383	Warner and Weiss (1985)
CFC-113	–136.129	206.474	55.8957	Bu and Warner (1995)
SF_6	–98.7264	142.803	38.8746	Bullister et al. (2002)
N_2O	–64.8539	100.252	25.2049	Weiss and Price (1980, p. 351)

where a_1, a_2, and a_3 are gas-species–specific constants and T is the temperature (in K). Values for a_1, a_2, and a_3 for the five gas species of interest in this study are provided in Table A2.

The Henry's Law coefficients should be expressed as air–water partitioning coefficients, K_w, in units of (g mol kg^{-1} water)/(g mole L^{-1} air), or L kg^{-1}, to evaluate gas-phase CFC transport through the vadose zone. Values of K_w may be computed from the equation

$$K_w = K_T RT \quad [A3]$$

where R is the ideal gas constant, 0.08205 atm L mol^{-1} K^{-1} or 8.314472 J mol^{-1} K^{-1}.

Acknowledgments

This study was supported by the USGS National Water-Quality Assessment (NAWQA) Program, High-Plains Regional Ground-Water Study, and the USGS National Research Program. The cooperation of landowners who agreed to the installation of monitoring equipment on their property is gratefully acknowledged. We particularly thank Kevin Dennehy (USGS, Reston, VA) and Bret Bruce, Jason Gurdak, and Jim Collins (USGS, Denver, CO) for their assistance with the installation and sampling of gas ports. We also acknowledge the contributions of two USGS colleague reviewers, Ed Busenberg and Robert Michel, for their helpful comments.

References

Bird, R.B., W.E. Stewart, and E.N. Lightfoot. 1960. Transport phenomena. McGraw-Hill, New York.

Bowden, W.B. 1986. Gaseous nitrogen emissions from undisturbed terrestrial ecosystems: An assessment of their impacts on local and global nitrogen budgets. Biogeochemistry 2:249–279.

Bowden, W.B., W.H. McDowell, C.E. Asbury, and A.M. Finley. 1992. Riparian nitrogen dynamics in two geomorphologically distinct tropical rain forest watersheds: Nitrous oxide fluxes. Biogeochemistry 18:77–99.

Brown, J.D. 1980. Evaluation of fluorocarbon compounds as ground-water tracers—soil column studies. M.S. thesis. Univ. of Arizona, Tucson.

Bu, X., and M.J. Warner. 1995. Solubility of chlorofluorocarbon 113 in water and seawater. Deep Sea Res. 42:1151–1161.

Bullister, J.L., D.P. Wisegarver, and F.A. Menzia. 2002. The solubility of sulfur hexafluoride in water and seawater. Deep Sea Res. 49:175–187.

Busenberg, E., and L.N. Plummer. 1992. Use of chlorofluorocarbons (CCl_3F and CCl_2F_2) as hydrologic tracer and age-dating tools: The alluvium and terrace system of central Oklahoma. Water Resour. Res. 28:2257–2283.

Busenberg, E., and L.N. Plummer. 2000. Dating young groundwater with sulfur hexafluoride: Natural and anthropogenic sources of sulfur hexafluoride. Water Resour. Res. 36:3011–3030.

Busenberg, E., E.P. Weeks, L.N. Plummer, and R.C. Bartholomay. 1993. Age dating ground water by use of chlorofluorocarbons (CCl_3F and CCl_2F_2) and distribution of chlorofluorocarbons in the unsaturated zone, Snake River Plain aquifer, Idaho National Engineering Laboratory, Idaho. Water Resour. Invest. Rep. 93-4054. USGS, Denver, CO.

Campbell, G.S. 1973. An introduction to environmental biophysics. Heidelberg Sci. Library. Springer Verlag, New York.

Cicerone, R.J. 1987. Changes in stratospheric ozone. Science 237:35–42.

Cook, P.G., and A.L. Herczeg. 2000. Environmental tracers in hydrology. Kluwer Acad. Press, Boston.

Cook, P.G., and D.K. Solomon. 1995. Transport of atmospheric trace gases to the water table: Implications for groundwater dating with chlorofluorocarbons and krypton 85. Water Resour. Res. 31:263–270.

Eichner, M.J. 1990. Nitrous oxide emissions from fertilized soils: Summary of available data. J. Environ. Qual. 19:272–280.

Engesgaard, P., A.L. Hojberg, K. Hinsby, K.H. Jensen, T. Laier, F. Larsen, E. Busenberg, and L.N. Plummer. 2004. Transport and time lag of chlorofluorocarbon gases in the unsaturated zone, Rabis Creek, Denmark. Vadose Zone J. 3:1249–1261.

Firestone, M.K., and E.A. Davidson. 1989. Microbiological basis of NO and N_2O production and consumption in soil. p. 7–21. *In* M.O. Andreae and

D.S. Schimel (ed.) Exchange of trace gases between terrestrial ecosystems and the atmosphere. Dahlem Worksh. Rep. 47. John Wiley & Sons, New York.

Goodroad, L.L., and D.R. Keeney. 1984. Nitrous oxide emission from forest, marsh, and prairie ecosystems. J. Environ. Qual. 13:448–452.

Healy, R.W. 1990. Simulation of solute transport in variably saturated porous media with supplemental information on modifications to the U.S. Geological Survey's computer program VS2D. Water Resour. Invest. Rep. 90-4025. USGS, Washington, DC.

Hill, M.C. 1998. Methods and guidelines for effective model calibration. Water Resour. Invest. Rep. 98-4005. USGS, Washington, DC.

International Atomic Energy Agency. 2006. Guidebook on the use of chlorofluorocarbons in hydrology. Int. Atomic Energy Agency, Vienna.

Kroeze, C., A.R. Mosier, and L. Bouwman. 1999. Closing the global N_2O budget: A retrospective analysis 1500–1994. Global Biogeochem. Cycles 13:1–7.

Letey, J., N. Valoras, D.D. Focht, and J.C. Ryden. 1981. Nitrous oxide production and reduction during denitrification as affected by redox potential. Soil Sci. Soc. Am. J. 45:727–730.

Massmann, J., and D.F. Farrier. 1992. Effects of atmospheric pressures on gas transport in the vadose zone. Water Resour. Res. 28:777–791.

Mathews, J.F. 1972. The critical constants of inorganic substances. Chem. Rev. 72:71.

McMahon, P.B., K.F. Dennehy, B.W. Bruce, J.K. Bohlke, R.L. Michel, J.J. Gurdak, and D.B. Hurlbut. 2006. Storage and transit time of chemicals in thick unsaturated zones under rangeland and irrigated cropland, High Plains, United States. Water Resour. Res. 42:W03413, doi:10.1029/2005WR004417.

McMahon, P.B., K.F. Dennehy, R.L. Michel, M.A. Sophocleous, K.M. Ellett, and D.B. Hurlbut. 2003. Water movement through thick unsaturated zones overlying the central High Plains aquifer, southwestern Kansas, 2000–2001. Water Resour. Invest. Rep. 03-4171. USGS, Reston, VA.

Menyailo, O.V., and B.A. Hungate. 2006. Stable isotope discrimination during soil denitrification: Production and consumption of nitrous oxide. Global Biogeochem. Cycles 20:GB3025, doi:10.1029/2005GB002527.

Millington, R.J. 1959. Gas diffusion in porous media. Science 130:100–102.

Monfort, J.P., and J.L. Pellegatta. 1991. Diffusion coefficients of the halogens CCl_2F_2 and $C_2Cl_2F_4$ with simple gases. J. Chem. Eng. Data 36:135–137.

Mosier, A.R., W.J. Parton, D.W. Valentine, D.S. Ojima, D.S. Schimel, and O. Heinemeyer. 1997. CH_4 and N_2O fluxes in the Colorado shortgrass steppe: 2. Long-term impact of land use change. Global Biogeochem. Cycles 11:29–42.

Osaka, K., N. Ohte, K. Koba, M. Katsuyama, and T. Nakajima. 2006. Hydrologic controls on nitrous oxide production and consumption in a forested headwater catchment in central Japan. J. Geophys. Res. 111: G01013, doi:10.1029/2005JG000026.

Parton, W.J., A.R. Mosier, D.S. Ojima, D.W. Valentine, D.S. Schimel, K. Weier, and A.E. Kulmala. 1996. Generalized model for N_2 and N_2O production from nitrification and denitrification. Global Biogeochem. Cycles 10:387–400.

Perry, J.H. (ed.) 1963. Perry's chemical engineers handbook. 4th ed. McGraw-Hill, New York.

Phillips, F.A., R. Luening, R. Baigent, K.B. Kelly, and O.T. Denmead. 2007. Nitrous oxide flux measurements from an intensively managed irrigated pasture using micrometeorological techniques. Agric. For. Meteorol. 143:92–107.

Poeter, E.P., and M.C. Hill. 1998. Documentation of UCODE: A computer code for universal inverse modeling. Water Resour. Invest. Rep. 98-4080. USGS, Denver, CO.

Reston Chlorofluorocarbon Laboratory. 2007. Air curve. Available at water.usgs.gov/lab/software/air_curve/ (verified 7 May 2007). USGS, Reston, VA.

Rochester, I.J. 2001. Estimating nitrous oxide emissions from flood-irrigated alkaline grey clays. Aust. J. Soil Res. 31:197–203.

Ronen, D., M. Magaritz, and E. Almon. 1988. Contaminated aquifers are a forgotten component of the global N_2O budget. Nature 335:57–59.

Santella, N., D.T. Ho, P. Schlosser, and M. Stute. 2003. Distribution of atmospheric SF_6 near a large urban area as recorded in the vadose zone. Environ. Sci. Technol. 37:1069–1074.

Santella, N., P. Schlosser, W.M. Smethie, D.T. Ho, and M. Stute. 2006. Seasonal variability and long term trends of chlorofluorocarbon mixing ratios in the unsaturated zone. Environ. Sci. Technol. 40:4414–4420.

Severinghaus, J.P., R.F. Keeling, B.R. Miller, R.F. Weiss, B. Deck, and W.S. Broecker. 1997. Feasibility of using sand dunes as archives of old air. J. Geophys. Res. 102:16783–16792.

Smith, K.A., H. Clayton, J.R.M. Arah, S. Christensen, P. Ambus, D. Fowler, K.J. Hargreaves, U. Skiba, G.W. Harris, F.G. Wienhold, L. Klemedtsson, and B. Galle. 1994. Micrometeorological and chamber methods for measurement of nitrous oxide fluxes between soils and the atmosphere: Overview and conclusions. J. Geophys. Res. 99:16541–16548.

Thornton, F.C., and R.J. Valente. 1996. Soil emissions of nitric oxide and nitrous oxide from no-till corn. Soil Sci. Soc. Am. J. 60:1127–1133.

Thorstenson, D.C., E.P. Weeks, H. Haas, and D.W. Fisher. 1983. Distribution of gaseous $^{12}CO_2$, $^{13}CO_2$, and $^{14}CO_2$ in the sub-soil unsaturated zone of the western U.S. Great Plains. Radiocarbon 25:315–346.

van Bavel, C.H.M. 1951. A soil aeration theory based on diffusion. Soil Sci. 72:33–46.

van Bochove, E., N. Bertrand, and J. Caron. 1998. In situ estimation of the gaseous nitrous oxide diffusion coefficient in a sandy loam soil. Soil Sci. Soc. Am. J. 62:1178–1185.

Walvoord, M.A., F.M. Phillips, D.A. Stonestrom, R.D. Evans, P.C. Hartsough, B.D. Newman, and R.G. Striegl. 2003. A reservoir of nitrate beneath desert soils. Science 302:1021–1024.

Warner, M.J., and R.F. Weiss. 1985. Solubilities of chlorofluorocarbons 11 and 12 in water and seawater. Deep Sea Res. 32:1485–1497.

Weast, R.C. (ed.). 1976. Handbook of chemistry and physics. 57th ed. CRC Press, Boca Raton, FL.

Weeks, E.P., D.E. Earp, and G.M. Thompson. 1982. Use of atmospheric fluorocarbons F-11 and F-12 to determine the diffusion parameters of the unsaturated zone in the southern High Plains of Texas. Water Resour. Res. 18:1365–1378.

Weiss, R.F., and B.A. Price. 1980. Nitrous oxide solubility in water and seawater. Mar. Chem. 8:347–359.

Werner, D., P. Grathwol, and P. Hohener. 2004. Review of field methods for the determination of the tortuosity and effective gas-phase diffusivity in the vadose zone. Vadose Zone J. 3:1240–1248.